G-protein signaling leverages subunit-dependent membrane affinity to differentially control βγ translocation to intracellular membranes

Patrick R. O'Neill[a], W. K. Ajith Karunarathne[a], Vani Kalyanaraman[a], John R. Silvius[b,1], and N. Gautam[a,c,1]

Departments of [a]Anesthesiology and [c]Genetics, Washington University School of Medicine, St. Louis, MO 63110; and [b]Department of Biochemistry, McGill University, Montreal, QC, Canada H3G 1Y6

Edited by Melvin I. Simon, University of California at San Diego, La Jolla, CA, and approved November 5, 2012 (received for review April 11, 2012)

Activation of G-protein heterotrimers by receptors at the plasma membrane stimulates βγ-complex dissociation from the α-subunit and translocation to internal membranes. This intermembrane movement of lipid-modified proteins is a fundamental but poorly understood feature of cell signaling. The differential translocation of G-protein βγ-subunit types provides a valuable experimental model to examine the movement of signaling proteins between membranes in a living cell. We used live cell imaging, mathematical modeling, and in vitro measurements of lipidated fluorescent peptide dissociation from vesicles to determine the mechanistic basis of the intermembrane movement and identify the interactions responsible for differential translocation kinetics in this family of evolutionarily conserved proteins. We found that the reversible translocation is mediated by the limited affinity of the βγ-subunits for membranes. The differential kinetics of the βγ-subunit types are determined by variations among a set of basic and hydrophobic residues in the γ-subunit types. G-protein signaling thus leverages the wide variation in membrane dissociation rates among different γ-subunit types to differentially control βγ-translocation kinetics in response to receptor activation. The conservation of primary structures of γ-subunits across mammalian species suggests that there can be evolutionary selection for primary structures that confer specific membrane-binding affinities and consequent rates of intermembrane movement.

protein–membrane interaction | spatio-temporal dynamics | G protein-coupled receptors

Compared with the vast biochemical information available for signaling proteins from cell-disruptive techniques, much less is known about their spatiotemporal dynamics in the 3D space of an intact living cell. Many important signaling proteins are posttranslationally modified with lipid groups that facilitate their interactions with membranes. Live cell imaging has so far revealed important roles for constitutive cycles that maintain proper localization of lipidated proteins (1) and for dynamic protein redistribution throughout the cell in response to a signal (2), but the detailed nature of lipid-modified protein movement between membranes is generally not well understood.

Heterotrimeric G proteins consist of lipid-modified α- and βγ-subunits (3). They are central transducers of the most important signaling pathways in mammals, yet little is known about their intracellular movement. Inactive heterotrimers consist of a GDP-bound α-subunit in complex with a stable βγ-dimer and localize to the plasma membrane (3). Extracellular signals activate transmembrane G-protein–coupled receptors (GPCRs) that catalyze nucleotide exchange on the G-protein α-subunit (3). The βγ-complex can then dissociate from the active α-subunit and translocate from the plasma membrane to intracellular membranes (4–6). βγ translocation has been observed for many different cell types and receptor types, suggesting that it is a common feature of G-protein signaling (4–8).

Two factors make βγ translocation an important model system for studying intermembrane movement of signaling proteins. First, the spatial redistribution of βγ-subunits within a cell is rapidly and reversibly driven by extracellular signals, facilitating kinetic analysis by live cell imaging (4, 6). Second, mammals express 5 β- and 12 γ-subunit types and the βγ-complex exhibits differential translocation kinetics that vary by over an order of magnitude, depending on the specific γ-subunit type (6, 8). The interactions responsible for these differential translocation kinetics are not known. Amino acid sequences vary significantly between different γ-subunits, but each is highly conserved across species, indicating their functional specificity. We used mutational approaches based on differences in evolutionarily conserved residues between γ-subunit types to identify the mechanistic basis of the translocation.

We used live cell imaging to investigate the reversible nature of βγ translocation as well as intermembrane exchange of free βγ during a continually stimulated cycle of G-protein activation. Our findings led to the development of a mathematical model of βγ translocation in which G-protein heterotrimers bind stably to the plasma membrane but free βγ-dimers dynamically interact with both the plasma membrane and intracellular membranes. Insight provided by this model motivated the hypothesis that direct interaction of the γ-subunit with lipid bilayers controls differential βγ translocation. Translocation kinetics of mutant γ-subunits, together with prenylated peptide rates of dissociation from lipid vesicles in vitro, supported this hypothesis and showed that hydrophobic and basic residues in the γ-subunit C-terminal domain determine βγ-membrane dissociation rates and translocation kinetics.

Results

Forward and Reverse βγ Translocations Have Similar γ-Subunit–Dependent Rates. In the classical model of the G-protein activation cycle (3), inactive $\alpha_{GDP}\beta\gamma$ heterotrimers reside at the plasma membrane. Receptor activation with an agonist triggers nucleotide exchange on the α-subunit and the α_{GTP} dissociates from βγ. Both α and βγ act on downstream effectors. GTP hydrolysis on the α-subunit, accelerated by interaction with GTP hydrolysis accelerating proteins (GAPs), deactivates the α-subunit and α_{GDP} reassembles with βγ. This cycle suggests γ-subunit dependence of three potential interactions to explain differential βγ-translocation rates: (*i*) the rate of heterotrimer dissociation, (*ii*) the rate at which βγ dissociates from the activated receptor, and (*iii*) the rate at which βγ dissociates from the plasma membrane. To help distinguish between these possibilities, we investigated the reversible nature of βγ translocation.

Receptor activation with an agonist triggers βγ translocation from the plasma membrane to intracellular membranes (4). The intracellular distribution of βγ-dimers is maintained in the

Author contributions: P.R.O., W.K.A.K., J.R.S., and N.G. designed research; P.R.O., W.K.A.K., and J.R.S. performed research; V.K. contributed new reagents/analytic tools; P.R.O., W.K.A.K., and J.R.S. analyzed data; and P.R.O., J.R.S., and N.G. wrote the paper.

The authors declare no conflict of interest.

This article is a PNAS Direct Submission.

[1]To whom correspondence may be addressed. E-mail: gautam@wustl.edu or john.silvius@mcgill.ca.

See Author Summary on page 20784 (volume 109, number 51).

This article contains supporting information online at www.pnas.org/lookup/suppl/doi:10.1073/pnas.1205345109/-/DCSupplemental.

continued presence of agonist, and βγ returns to the plasma membrane on receptor deactivation with an antagonist (4, 6). The reverse rates have not been studied in detail. We therefore measured forward and reverse βγ-translocation rates for three different γ-subunits. HeLa cells were transfected with untagged αo, β1, and a fluorescent protein (FP)-tagged γ-subunit (γ9, γ5, or γ3) and imaged by spinning-disk confocal microscopy (Fig. 1). We recently used fluorescence complementation to show that FP-tagged γ-subunits can be used to accurately measure the translocation kinetics of βγ-dimers, consistent with the well-known stable association of β- and γ-subunits under physiological conditions (8). Endogenous Gi/o-coupled α2 adrenergic receptors (α2ARs) were activated with 10 μM norepinephrine (agonist) to stimulate forward βγ translocation and deactivated with 60 μM yohimbine (antagonist) to stimulate reverse translocation. For each γ-subunit, the reverse translocation rate was similar to the forward rate. Fast-translocating γ9 returned quickly on receptor deactivation, and slower-translocating γ5 and γ3 returned more slowly (Fig. 1*B*). Similar results were obtained on activation and deactivation of endogenous Gi/o-coupled CXCR4 receptors with SDF-1α (CXCL12, agonist) and AMD-3100 (antagonist), respectively (Fig. S1 and Movies S1 and S2). These results suggested that both forward and reverse translocations share the same γ-subunit–dependent rate-limiting step and raised the possibility that γ-dependent rates of βγ-dissociation from lipid bilayers may explain the differential βγ-translocation kinetics.

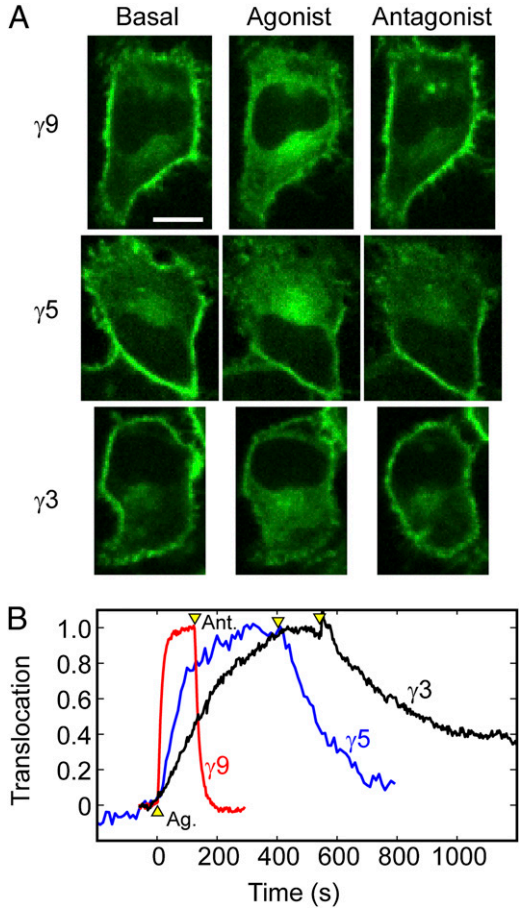

Fig. 1. Reverse βγ-translocation rates show the same γ-subunit dependence as forward translocation rates. (*A*) Confocal images of HeLa cells transfected with αo, β1, and FP-tagged γ9, γ5, or γ3. Forward βγ translocation was triggered by activation of endogenous α2AR with 10 μM norepinephrine (agonist). Reverse translocation was triggered by receptor deactivation with 60 μM yohimbine (antagonist). (*B*) Corresponding forward and reverse translocation kinetics for γ9, γ5, and γ3. Arrowheads mark the addition of agonist and antagonist. To facilitate direct comparison of kinetics, we defined "translocation" as the increase in intracellular fluorescence intensity stimulated by receptor activation, normalized by the maximum intracellular intensity reached. Here and in subsequent figures, images labeled "basal" were captured shortly before agonist addition, and images labeled "agonist" or "antagonist" were captured at some time point after forward or reverse translocation reached steady state. (Scale bar: 20 μm.)

Free βγ Dimers Diffuse Throughout the Cell, Exploring both the Plasma Membrane and Intracellular Membranes. Next we examined the steady-state intermembrane dynamics of free βγ-subunits to determine whether they were consistent with the possibility that membrane dissociation rates determine βγ-subunit translocation rates. The ability of intracellular βγ to return rapidly to the plasma membrane on receptor deactivation suggests that free βγ, which is not bound to the α-subunit, continually explores the cytosolic surfaces of both intracellular membranes and the plasma membrane. Fluorescence recovery after photobleaching (FRAP) in the presence of agonist was used to test whether free βγ shuttles between membranes (Fig. 2). HeLa cells were transfected with αo, β1, and a representative slow (GFP-γ3) or fast γ-subunit type (GFP-γ9) and imaged. βγ translocated to intracellular membranes on activation of endogenous CXCR4 receptors with SDF-1α (Fig. 2 *A* and *B*). When the intracellular βγ distribution reached a steady state, we photobleached an intracellular membrane region. We then monitored fluorescence intensity at both the bleached intracellular region and an unbleached region of the plasma membrane, in the continued presence of SDF-1α to maintain a steady pool of free βγ (Fig. 2 *A* and *C*). Fluorescence loss from the plasma membrane accompanied the fluorescence recovery at the intracellular membrane, and single exponential fits yielded similar time constants of 8.3 s and 13.9 s (Fig. 2*C*). The loss of plasma membrane fluorescence suggests the exchange of fluorescent (unbleached) βγ from the plasma membrane with photobleached βγ from the intracellular membrane region. This result implies that βγ-dimers released by sustained cycles of G-protein activation move continually between the different membranes. In the presence of agonist, FRAP recovery in a bleached region of intracellular membranes showed the same γ-dependence as the translocation rates from the plasma membrane to intracellular membranes, with fast recovery for γ9 and much slower recovery for γ3 (Fig. 2 *D* and *E*). Similar results were observed when endogenous α2 adrenergic receptors were activated instead of CXCR4 (Fig. S2). Thus, free βγ-dimers continually explore both the plasma membrane and intracellular membrane surfaces, moving at γ-dependent rates that determine their differential forward and reverse translocation in response to an extracellular signal.

Mathematical Model Reproduces γ-Subunit–Dependent Forward and Reverse Translocation Kinetics with a Single Free Parameter. Guided by the reversible nature of βγ translocation and shuttling of free βγ, we developed a model describing the key interactions controlling βγ translocation. The model is based on three main assumptions (Fig. 3):

i) Association/dissociation with the α-subunit is the switch that controls βγ translocation. Both the α- and γ-subunits of G-protein heterotrimers are modified with lipid groups (9). The α-subunits are palmitoylated and/or myristoylated, depending on the specific α-subtype. The γ-subunits are prenylated with either a 15-carbon farnesyl (γ1, γ9, and γ11) or a 20-carbon geranylgeranyl (all other γ-subunit types) (9). Activated receptors catalyze nucleotide exchange on the α-subunit from α_{GDP} to α_{GTP} and dissociation from the βγ-complex. Because heterotrimers bind with at least two lipidic groups to the plasma membrane (9), whereas free βγ-dimers bind with a single prenyl moiety (9), dissociation of free βγ from the plasma membrane is likely much faster than that of heterotrimers. This assumption is consistent with reports that doubly lipidated proteins dissociate from membranes on the timescale of 100 h (10) whereas singly prenlyated proteins dissociate in minutes or less (11).

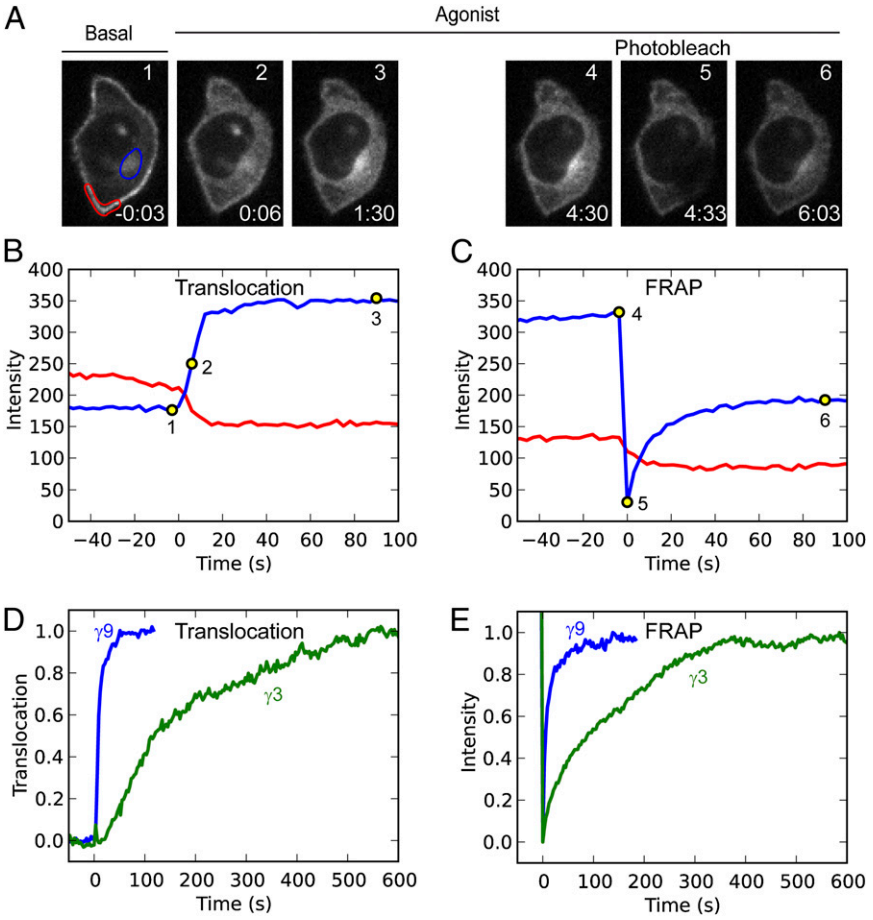

Fig. 2. Free βγ-subunits interact dynamically with membranes. (*A*) Live cell confocal images of a HeLa cell transfected with αo, β1, and GFP-γ9. Images *1–3*: βγ translocation stimulated by activation of endogenous CXCR4 receptors with 100ng/mL SDF-1α. Images *4–6*: After the βγ distribution reached a steady state, in the presence of SDF-1α, an intracellular membrane region was photobleached and the recovery in this region was monitored. The time for each image, relative to the addition of SDF-1α, is given in min:s. (*B* and *C*) Fluorescence intensity changes at the plasma membrane (red) and intracellular membrane (blue) regions as defined in *A*, corresponding to translocation (*B*) and FRAP (*C*). (*D*) Representative translocation kinetics for γ9 and γ3. (*E*) Representative FRAP recovery kinetics for γ9 and γ3.

ii) Free βγ-dimers diffuse throughout the cell, exploring both the plasma membrane and intracellular membranes. The above FRAP studies in the presence of agonist strongly support this assumption. It is also consistent with observations that prenylated proteins lacking a "second signal," such as an additional lipid modification or a polybasic domain, associate dynamically with membranes (12).

iii) γ-Dependent translocation rates result from differential membrane dissociation rates determined by the C-terminal domain of the γ-subunit. Previous studies showed that βγ-translocation rates are primarily determined by the C-terminal domain of the γ-subunit (6, 13). On the basis of evidence for direct interaction of the C-terminal domain of the γ-subunit with a GPCR, those results were thought to imply that differential translocation rates are determined by βγ release from the receptor following G-protein activation (13). However, the differential return translocation of βγ to the plasma membrane following receptor deactivation, along with the known role for the prenylated γ-subunit C-terminal domain in βγ-membrane interactions (14), suggests an alternative explanation where residues in the C-terminal domain of the γ-subunit influence the membrane dissociation rates of the βγ-complex through direct interaction with lipid membranes.

To generate quantitative predictions based on these assumptions, we developed a mathematical model that included the classical steps of the G-protein activation cycle, modified by treating the plasma membrane and intracellular membranes as two distinct compartments with rate constants k_{in} and k_{out} describing exchange of βγ-subunits between them (Fig. 4*A*). This approach allowed for a simple kinetic model without the need for more detailed modeling of cell geometry, βγ-membrane dissociation rates, or diffusion between membranes. Those factors are implicitly contained in k_{in} and k_{out}. Because the concentration of αo at the plasma membrane does not change on receptor activation (4), the total concentration of α-subunits, $[\alpha_{GTP}] + [\alpha_{GDP}] + [\alpha_{GDP}\beta\gamma]$, at the plasma membrane was held constant. Treatment of the classical steps of G-protein signaling, including (*i*) the rate of association of α_{GDP} with βγ, (*ii*) the rate of heterotrimer activation/dissociation, and (*iii*) the rate of GAP-induced GTP hydrolysis on the α-subunit, followed a previous study of G-protein signaling kinetics (15). This facilitated the use of appropriate parameter values collected from the literature for concentrations of receptors, G proteins, and GAPs and rate constants for G-protein activation/dissociation, GAP accelerated GTP hydrolysis, and heterotrimer reassociation (15) (see *Methods* for equations and parameter values).

Analogous to the sequential addition of agonist and antagonist used to measure forward and reverse translocation rates in live cells, we simulated translocation in the model by changing the concentration of activated receptors from 0 to 30 nM at the time corresponding to agonist addition and back to 0 at the time corresponding to antagonist addition. The specific value used for the concentration of activated receptors did not significantly influence the translocation kinetics discussed here (Fig. S3). Model-generated translocation curves were compared with translocation data for γ9, γ5, and γ3 from HeLa cells sequentially treated with norepinephrine and yohimbine (Fig. 4*B*). To generate simulated curves that best fitted the data, k_{in} and k_{out} were varied with all other parameters fixed to values from the literature (15). Notably, the best fits for all three subunits were obtained with $k_{in} = k_{out}$ (0.05 s^{-1} for γ9, 0.006 s^{-1} for γ5, and 0.0025 s^{-1} for γ3), indicating that a single free parameter was sufficient to model the differential forward and reverse βγ-translocation kinetics. This finding suggests that the same rate-limiting step determines both inward and return

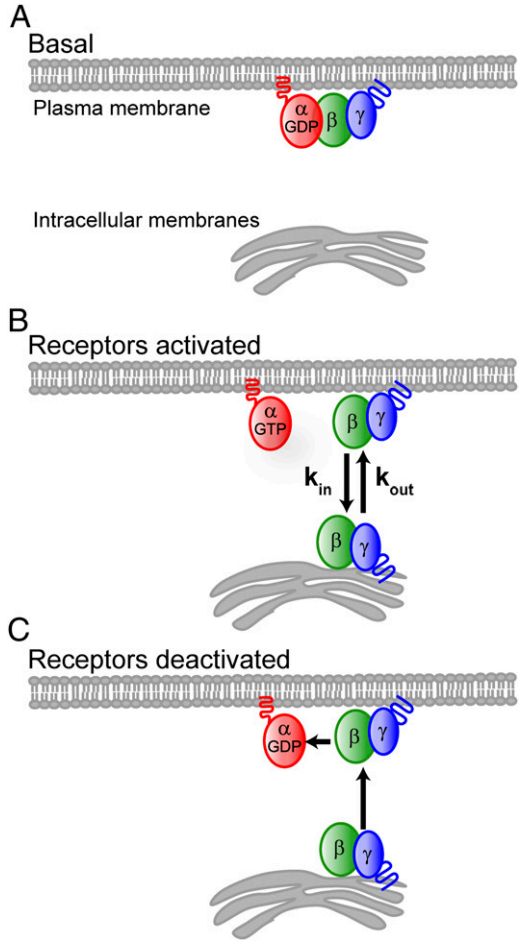

Fig. 3. Model for βγ translocation. (*A*) Heterotrimers with lipidated α- and γ-subunits interact stably with the plasma membrane. (*B*) On receptor activation, the βγ-complex dissociates from the α-subunit. The single prenyl moiety on the γ-subunit facilitates membrane interaction but is insufficient for stable membrane binding of βγ, which diffuses throughout the cytosol and binds transiently to both the plasma membrane and intracellular membranes. A pool of free βγ is available to participate in the G-protein activation cycle at the plasma membrane as long as receptors are active. (*C*) On receptor deactivation, $\alpha_{GDP}\beta\gamma$ heterotrimers rapidly accumulate at the plasma membrane, depleting the intracellular pool of βγ.

translocation rates, consistent with our hypothesis that membrane dissociation rates determine differential βγ-translocation kinetics.

Mutagenesis Reveals That Hydrophobic and Positively Charged Residues in the γ-Subunit C-Terminal Domain Determine βγ-Translocation Rates. We then examined the possibility that translocation and shuttling rates are determined by direct interaction of the γ-subunit with lipid membranes. The 12 mammalian γ-subunits can be grouped into fast- (~10 s), intermediate- (~50 s), and slow (~130 s)-translocating subunits (8). An examination of their C-terminal domains reveals that each of the slowest-translocating γ-subunits (γ2, γ3, and γ4) has the same C-terminal domain (Fig. 5): EKKFFCALL, which becomes EKKFFC(GerGer) after posttranslational modification at the endoplasmic reticulum, where the prenylated cysteine is also methylated (9). Given the positioning of the hydrophobic phenylalanines and the positively charged lysines with respect to the prenylated cysteine, we predicted that the hydrophobic residues enhance the hydrophobic interaction with the membrane and the positively charged residues contribute an electrostatic attraction to negatively charged lipid head groups, thus slowing βγ dissociation from the membrane.

We tested the influence of these residues on βγ translocation in HeLa cells coexpressing αo, β1, and GFP-tagged γ-subunit mutants (Fig. 6 and Table 1). As in the case of the wild-type subunits, translocation rates of mutant γ-subunits did not depend on whether endogenous α2AR or CXCR4 receptors were activated (Table 1). We separately tested the role of hydrophobic and positively charged residues by mutating the C-terminal domain of γ3 from EKKFFC(GerGer) to either EKK**AA**C(GerGer) or E**AA**FFC(GerGer), respectively (mutated residues marked in boldface). Both mutants showed markedly faster translocation than wild-type γ3, with the half-time reduced from ~130 s to ~35 s. The γ3 mutant ending in EAAAAC(GerGer) translocated still

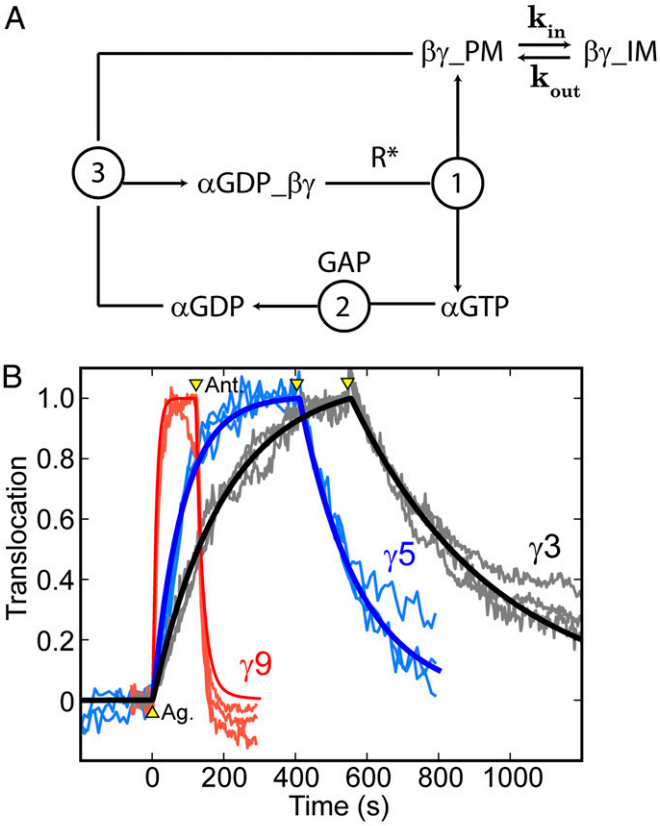

	k_in = k_out	$t_{1/2}$ (F)	$t_{1/2}$ (R)
γ9	0.05 s^{-1}	9 s	16 s
γ5	0.006 s^{-1}	59 s	117 s
γ3	0.0025 s^{-1}	128 s	280 s

Fig. 4. Mathematical model suggests that the same rate-limiting step controls forward and reverse translocation. (*A*) Schematic showing the processes considered by the model, including (*1*) heterotrimer activation/dissociation catalyzed by activated receptors (R*), (*2*) GAP accelerated GTP hydrolysis by the α-subunit, and (*3*) reassociation of βγ with α_{GDP}. Additionally, the model allows for βγ exchange between the plasma membrane (PM) and intracellular membranes (IM) by considering them as two different compartments. (*B*) Live cell translocation data for three cells each for γ9 (red), γ5 (blue), and γ3 (gray), including data from Fig. 1*B*. Translocation curves generated from the model are plotted on top of the live cell data. Arrowheads mark the addition of agonist and antagonist. With the exception of k_{in} and k_{out}, all other parameters were obtained from the literature and fixed at the same values for all three fits. The model reproduced the forward and reverse translocation kinetics of all three γ-subunits, using just a single free parameter ($k_{in} = k_{out}$), suggesting that forward and reverse translocations share the same rate-limiting step. The values of k_{in} (= k_{out}) used to generate translocation curves from the model are displayed below, along with the resulting $t_{1/2}$ values for forward (F) and reverse (R) translocation.

Fast Translocating ($t_{1/2}$ ~ 10 s)

γ1 --NPFKELKGGCVIS
γ9 --NPFKE-KGGCLIS
γ11 --NPFKE-KGSCVIS

Intermediate ($t_{1/2}$ ~ 60 s)

γ5 --NPFRPQKV-CSFL
γ7 --NPFKDKKP-CIIL
γ10 --NPFREPRS-CALL
γ12 --NPFKDKKT-CIIL
γ13 --NPWVE-KGKCTIL

Slow Translocating ($t_{1/2}$ ~ 130 s)

γ2 --NPFREKKFFCAIL
γ3 --NPFREKKFFCALL
γ4 --NPFREKKFFCTIL
γ8 --NPFRDKRLFCVLL

Fig. 5. Slowest-translocating γ-subunits share the same C-terminal domain. Shown is sequence alignment of γ-subunit C-terminal domain sequences, grouped by translocation rates. Three of the four slowest-translocating subunits (γ2, -3, and -4) share the same KKFFC(GerGer) C-terminal sequence, and the fourth (γ8) also contains two basic residues, two hydrophobic residues, and a geranygeranylated cysteine.

faster with a $t_{1/2}$ of ~20 s. A γ9 mutant with C-terminal domain EKKFFC(Farn) translocated with $t_{1/2}$ of ~20 s, as did a γ3 mutant with an identical C-terminal domain, compared with ~10 s for wild-type γ9 with C-terminal domain EKGGC(Farn). Clearly, hydrophobic and positively charged residues strongly influence the translocation rates of geranylgeranylated βγ-subunits. Intracellular FRAP was also performed on mutant γ-subunits in the presence of agonist. Consistent with results from wild-type subunits, FRAP recovery rates for mutant γ-subunits correlated with translocation rates in a γ-dependent manner (Fig. S2). Together, the FRAP recovery and translocation kinetics of mutant γ-subunits suggest that hydrophobic and basic residues in the C-terminal domain of geranylgeranylated subunits determine βγ-translocation rates by tuning membrane dissociation rates.

Same Residues That Determine βγ-Translocation Rates Directly Control Membrane Dissociation Rates in Vitro. To test whether hydrophobic and basic residues that strongly influence βγ-translocation rates in live cells also directly influence interaction with lipid membranes, we measured peptide dissociation from lipid vesicles in vitro (Table 2). Fluorescently labeled pentapeptides corresponding to prenylated and cysteine *O*-methylated C-terminal sequences of γ-subunits were chemically synthesized, and their dissociation rates from lipid vesicles were measured by a previously described fluorimetric method (11, 16, 17). The peptides were methylated because the prenylated cysteines in the corresponding native proteins are known to be methylated (9). We synthesized peptides corresponding to the C-terminal sequences of wild-type γ3 and γ9 and peptides corresponding to mutations of the basic and hydrophobic residues.

At 37 °C, the peptide corresponding to the C-terminal domain of wild-type γ3, KKFFC(GerGer)-OMe, dissociated from PC/PE/PS/cholesterol (35/35/30/50) vesicles with a half-time of ~240 s. A single-residue change to **E**KFFC(GerGer)-OMe resulted in much faster dissociation with a half-time of ~12 s. The peptide **EKGG**C(GerGer)-OMe, which lacked both the second lysine and the two phenylalanines, dissociated with a still faster half-time of ~0.6 s. Farnesylated versions of these three peptides dissociated much faster than their geranylgeranylated counterparts (Table 2). The C-terminal domain of wild-type γ9, EKGGC(Farn)-OMe, dissociated with a half-time shorter than the temporal resolution limit for our assay (<0.14 s). The half-time for dissociation of the phenylalanyl-substituted species EK**FF**C(Farn)-OMe was significantly longer (~0.3 s), and additional replacement of the glutamic acid residue to yield **KKFF**C(Farn)-OMe further increased the half-time to ~2.4 s. These results indicate that hydrophobic and positively charged residues, along with the more hydrophobic geranylgeranyl lipid moiety, all contribute significantly to reducing the rate of membrane dissociation of slower-translocating γ-subunits (e.g., γ3) compared with that of faster-translocating γ-subunits such as γ9. The effects of these residues on membrane dissociation rates thus qualitatively mirror the pattern of translocation rates observed for different βγ-subunits in cells and quantitatively are sufficiently large to account for the magnitudes of the observed differences in βγ-translocation rates in vivo.

For the prenylated peptides just discussed, the rates of bilayer dissociation show an even stronger dependence on the amino acid sequence and the nature of the attached prenyl group than was observed for the rates of translocation of different γ-subunits

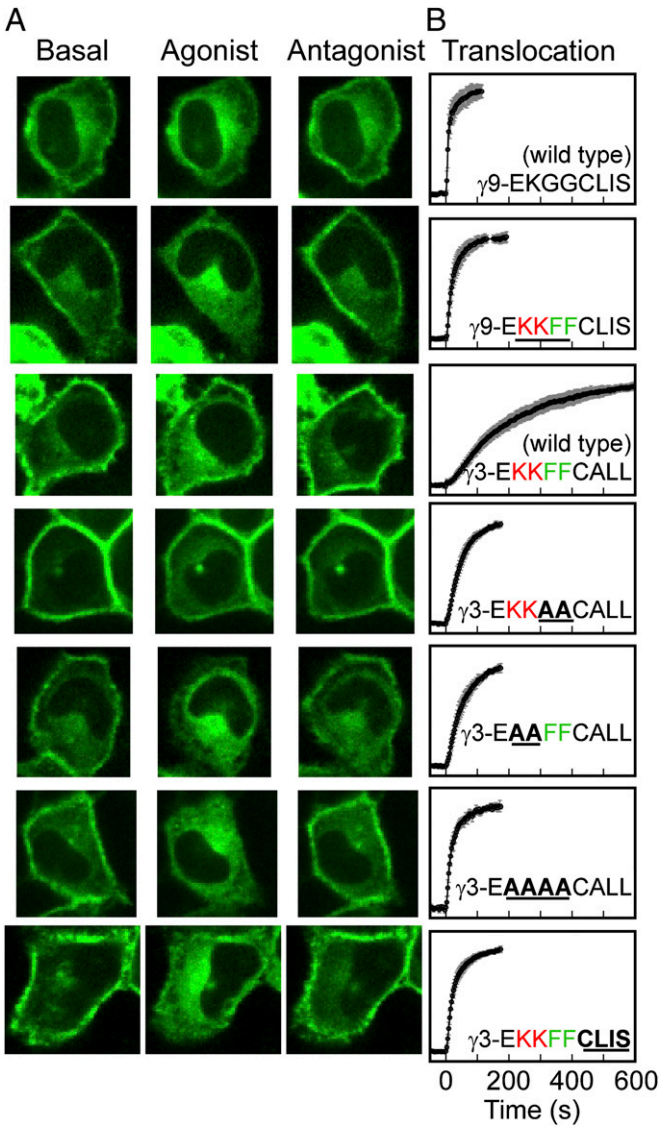

Fig. 6. Hydrophobic and positively charged residues in the γ-subunit C-terminal domain determine rate of βγ translocation. (*A*) Confocal images of HeLa cells transfected with αo, β1, and a wild-type or mutant GFP-tagged γ-subunit. The specific γ-subunits are specified in the corresponding plots of the forward translocation kinetics in *B*. Data are plotted as the mean (±SD) from at least $n = 14$ cells and three independent experiments. Agonist addition corresponds to $t = 0$ s.

Table 1. Translocation kinetics for wild-type and mutant γ-subunits

γ-Subunit	Half-time for translocation, s	
	α2 adrenergic	CXCR4
γ9-E-KGGCLIS, wild type	9.0 ± 1.7 (22)	8.4 ± 1.2 (14)
γ9-EKKFFCLIS	16.5 ± 0.7 (31)	18.7 ± 1.4 (19)
γ3-EKKFFCALL, wild type	124 ± 17 (8)	129 ± 8 (23)
γ3-EKKAACALL	31.4 ± 1.7 (36)	34.2 ± 2.3 (23)
γ3-EAAFFCALL	37.8 ± 1.9 (29)	36.1 ± 1.6 (18)
γ3-EAAAACALL	20.6 ± 4.3 (22)	18.9 ± 4.4 (18)
γ3-EKKFFCLIS	15.7 ± 0.9 (26)	18.5 ± 0.6 (32)

Sequences correspond to the C-terminal regions of the subunits. Translocation half-times are given as the mean ± SEM (number of cells in parentheses) from at least three independent experiments. Residues of interest are in boldface: positively charged (red), hydrophobic (green), mutations (black, underlined).

in living cells. Several factors may contribute to this difference. First, computational studies (18) suggest that the β1γ1 complex interacts with phospholipid membranes not only through the prenylated carboxy terminus of the γ-subunit but also through a cluster of basic residues on the β-subunit. The electrostatic contribution from the β-subunit may reduce the membrane dissociation rates for βγ-dimers compared with those for the prenylated γ-derived peptides. This contribution may be especially important for farnesylated βγ, where the lipid moiety alone provides limited membrane affinity. Alternatively, membrane dissociation may not be the sole rate-limiting process for translocation of rapidly dissociating farnesylated βγ-subunits. For example, on the basis of the rates of cytosolic diffusion measured for GFP constructs of various molecular weights in *Escherichia coli* (19), we estimate that for GFP-tagged βγ, root-mean-square displacements within the cytosol of 5 μm, 10 μm, and 20 μm would require roughly 0.6 s, 2.3 s, and 9.5 s, respectively (*SI Text*). The possibility that diffusion through the cytosol becomes rate limiting for the translocation of farnesylated βγ-dimers is consistent with the observation that translocation half-times for farnesylated βγ-dimers in cells are longer than bilayer dissociation rates for farnesylated peptides in vitro. The possibility just noted might also explain the relatively small effect of mutating EKGGC(Farn) to KKFFC(Farn) on βγ9 translocation in cells. Finally, protein chaperones may exist that facilitate removal of prenylated βγ from membranes. Many such proteins are known to act on prenylated small GTPases (20–22), and phosducin is known to facilitate βγ translocation in photoreceptors by diminishing its membrane partitioning (23, 24). It is unknown whether chaperones regulate βγ translocation in other cell types. Overall, however, the results presented here indicate that the translocation rates of different βγ-subunits reflect membrane dissociation rates that are determined by the nature of the prenyl group and by basic and hydrophobic residues in the γ-subunit C-terminal domain.

γ-Dependent Translocation Kinetics Hold for Multiple α- and β-Subunit Types. The role we have shown for the γ-subunit interaction with membranes in determining the differential translocation kinetics suggests that the same γ-dependent kinetic pattern should also hold for other α- and β-subunit types besides αo and β1. To test whether the γ-dependent translocation pattern occurs with heterotrimers containing other α-subunits, we imaged translocation of βγ containing different γ-subunit types in HeLa cells cotransfected with Gs-coupled D1 dopamine receptors (Fig. 7*A*). The translocation rates show that translocation triggered by activation of Gs heterotrimers yields the same γ-dependent kinetics observed for activation of Go heterotrimers (Fig. 7*B*). This result is consistent with a previous report that γ11 translocation can be stimulated by activation of Gs-, Gi-, and Gq-coupled receptors (5). We then used a fluorescence complementation assay to test whether the γ-dependent translocation rates occur in complex with other β-subunits. Translocation of βγ-dimers composed of β2 and γ9, γ5, or γ2 was measured in HeLa cells transfected with αo, $Venus_{156–239}$-β2, and the corresponding $Venus_{1–155}$-γ on activation of endogenous α2AR (Fig. 7*C*). γ2 has the same C-terminal domain and translocation kinetics as γ3. All three combinations formed fluorescent βγ-dimers, and their translocation kinetics showed that βγ-complexes composed of β2 exhibit the same γ dependence as those composed of β1 (Fig. 7*D*). Altogether the results show that the differential βγ-translocation rates hold for multiple α- and β-subunit types.

Differential Translocation Kinetics Hold for Multiple FP-Tagged γ-Subunits in the Same Cell. Because most cells express multiple γ-subunit types, we tested whether the same γ-dependent translocation kinetics hold when multiple FP-tagged γ-subunits are expressed in the same cell. In HeLa cells coexpressing YFP-γ9 and mCherry-γ3, βγ-dimers composed of either γ-subunit type translocated on activation of endogenous CXCR4 receptors (Fig. 8*A*). The corresponding translocation plots (Fig. 8*B*) show that the different γ-subunit types exhibit the same differential translocation kinetics whether they are expressed individually or together in the same cell.

βγ Translocation Exhibits Consistent γ-Subunit–Dependent Kinetics over a Wide Range of GFP-γ-Subunit Expression Levels. To examine whether the expression level of a GFP-tagged γ-subunit influenced the translocation kinetics, we transfected HeLa cells with one of three GFP-γ subunits (γ9, γ3, or γ3-EAAFFCALL) and assayed cells with a wide range of GFP-γ-subunit expression levels. Using our imaging system, which is equipped with a highly sensitive EMCCD camera, we measured translocation kinetics in cells expressing the lowest detectable level of GFP-γ. We then measured translocation kinetics in cells with various expression levels up to 60-fold higher than the lowest detection limit (details in *Methods*). Cells with expression levels above this range were not studied because GFP-γ did not properly localize to the plasma membrane. The results (Fig. 9) show that the βγ-translocation kinetics are determined by the γ-subunit type

Table 2. In vitro membrane dissociation kinetics for peptides corresponding to the C-terminal domain of wild-type and mutant γ-subunits

Peptide sequence	Half-time for dissociation, s		
	PC/PE/PS, 20 °C	PC/PE/PS/Ch, 20 °C	PC/PE/PS/Ch, 37 °C
EKGGC(farnesyl)-OMe	0.20 ± 0.02	<0.14	<0.14
EKFFC(farnesyl)-OMe	0.74 ± 0.03	0.40 ± 0.05	0.30 ± 0.03
KKFFC(farnesyl)-OMe	7.0 ± 0.2	3.2 ± 0.2	2.4 ± 0.1
EKGGC(geranylgeranyl)-OMe	1.8 ± 0.2	1.1 ± 0.1	0.58 ± 0.04
EKFFC(geranylgeranyl)-OMe	59 ± 6	26 ± 1	12.5 ± 0.8
KKFFC(geranylgeranyl)-OMe	638 ± 24	368 ± 30	240 ± 21

Half-times are given as the mean ± SEM for three independent experiments. Membrane compositions: PC/PE/PS, 37.5/37.5/37.5; PC/PE/PS/cholesterol, 35/35/30/50.

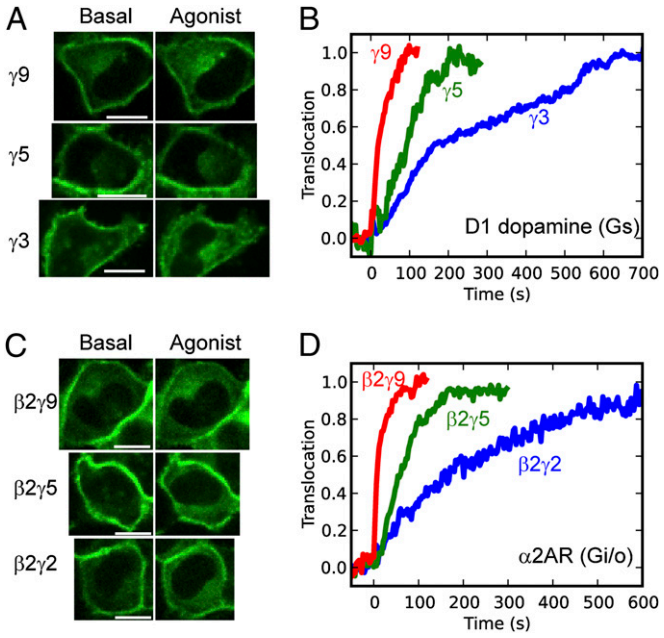

Fig. 7. γ-Dependent translocation kinetics hold for multiple α- and β-subunit types. (*A*) Confocal images of HeLa cells transfected with D1 dopamine receptors and FP-γ9, -γ5, or -γ3 subunits. Gs heterotrimers were activated by stimulation of D1 receptors with 1 μM A68930. (*B*) Translocation kinetics corresponding to the cells shown in *A*. (*C*) Confocal images of HeLa cells coexpressing αo, $Venus_{156–239}$-β2, and one of three different $Venus_{1–155}$-tagged γ-subunits. Endogenous α2ARs were stimulated with 10 μM norepinephrine. (*D*) Translocation kinetics corresponding to the cells shown in *C*. Agonist addition corresponds to $t = 0$ s. (Scale bars: 20 μm.)

and not the expression level. This finding shows that the differential kinetics are not due to overexpression of γ-subunits and suggests that endogenous γ-subunits differ in translocation rates similarly. It is also consistent with βγ-translocation rates being determined directly by membrane dissociation rates.

Discussion

Cell-signaling networks commonly use proteins capable of reversible membrane targeting (25, 26). Recent systems biological approaches have provided examples of how information encoded in the spatiotemporal activity of such proteins can be integrated by key signaling proteins such as ERK to produce a stimulus-dependent cellular response (27–29). These findings highlight the need for a detailed understanding of the molecular mechanisms governing intracellular protein movement. Reversible membrane targeting is typically achieved either by protein domains that bind specifically to low-abundance "signaling" lipids whose membrane concentrations vary in response to cellular stimuli (30) or by posttranslational modification with hydrophobic fatty acids and/or prenyl groups that facilitate membrane binding (31). A single protein-linked acyl or prenyl group acting alone typically confers rapidly reversible, relatively nonselective membrane binding and must be combined with a second membrane-targeting element to achieve high stability or specificity of binding to membranes (31–34). For example, prenylated proteins including G-protein heterotrimers and small G proteins often contain a reversible second membrane-targeting element in the form of either a palmitoyl group or a polybasic domain (33, 35).

The ability of G-protein βγ-subunits to translocate at different rates between the plasma membrane and intracellular membranes in direct response to extracellular signals makes G-protein heterotrimers a particularly attractive model to understand intracellular protein movement of lipid-modified proteins. We therefore performed a detailed study to determine the key molecular mechanisms that control βγ translocation. We found that the prenylated βγ-complex interacts dynamically with membranes when dissociated from the lipidated α-subunit, constantly moving between the plasma membrane and intracellular membranes. This free βγ movement between various membranes is consistent with the general requirement of a second signal for stable membrane binding of prenylated proteins (12, 31) and with reports that βγ-subunits require coexpression of the α-subunit for targeting to the plasma membrane (36–38). It is also consistent with reports that geranylgeranylated as well as farnesylated peptides show rapid membrane dissociation kinetics in vitro (11). Motivated by the finding that the forward and reverse βγ-translocation rates as well as the free βγ-shuttling rates exhibit the same γ dependence, we developed a mathematical model to describe βγ translocation. In the model, the combined lipid modifications on the α- and γ-subunits stably bind heterotrimers to the plasma membrane. G-protein activation by a receptor triggers heterotrimer dissociation, and free βγ dissociates from the plasma membrane and redistributes over intracellular membranes, continually testing the surfaces of both intracellular membranes and the plasma membrane. In this way free βγ maintains a steady intracellular pool while still monitoring the plasma membrane, where it is available to bind inactive α_{GDP} and facilitate continued cycles of nucleotide exchange on the α-subunit. As long as agonist-bound receptors maintain the rate of heterotrimer activation at a sufficient level, a steady-state intracellular pool of βγ is actively maintained. Receptor deactivation stops heterotrimer activation, resulting in relocalization of βγ to the plasma membrane in $\alpha_{GDP}\beta\gamma$ heterotrimers. Simulations using this model required just a single γ-dependent free parameter to fit forward and reverse translocation kinetics of fast-, intermediate-, and slow-translocating γ-subunits, suggesting that

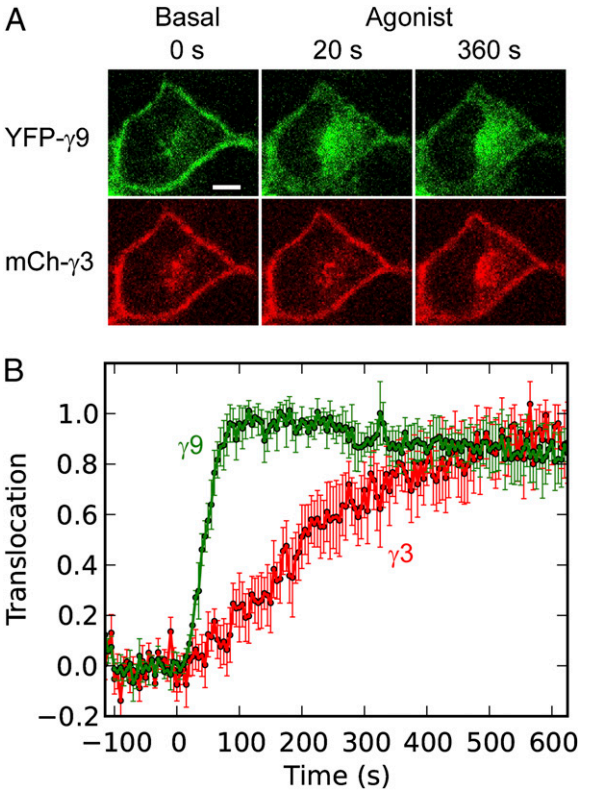

Fig. 8. Differential translocation kinetics hold for multiple γ-subunit types expressed in the same cell. (*A*) Confocal images of a HeLa cell expressing both YFP-γ9 and mCherry-γ3, showing differential translocation on activation of endogenous CXCR4 receptors with 100 ng/mL SDF-1α. (*B*) Corresponding translocation kinetics. Data are plotted as the mean (±SD) for $n = 8$ cells. Agonist addition corresponds to $t = 0$ s. (Scale bar: 10 μm.)

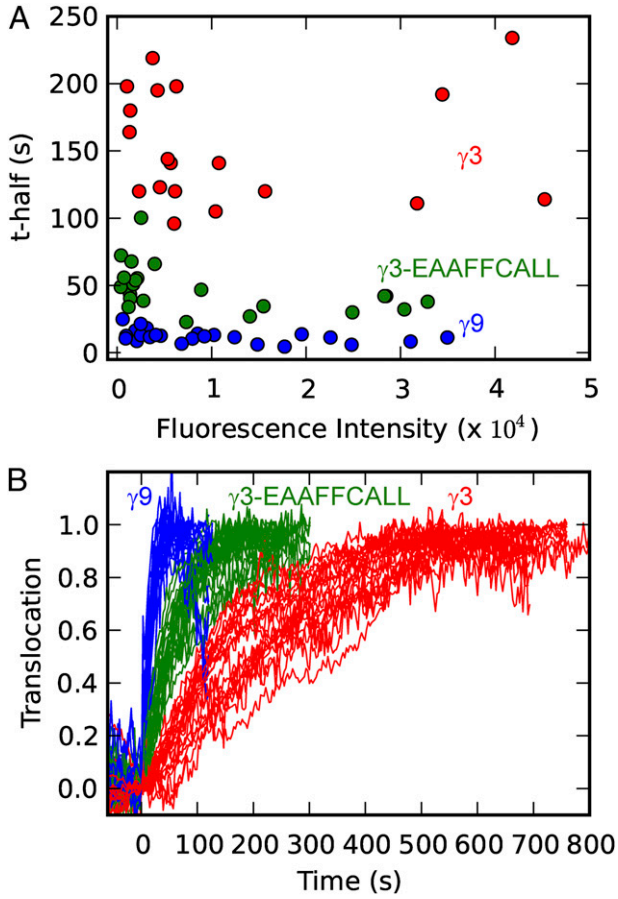

Fig. 9. βγ translocation exhibits consistent γ-subunit–dependent kinetics over a wide range of GFP-γ expression levels. (*A*) Dependence of the translocation rate ($t_{1/2}$) on the mean fluorescence intensity in HeLa cells transfected with GFP-tagged γ9, γ3, or γ3-EAAFFCALL. (*B*) Translocation curves corresponding to the data in *A*. Endogenous α2ARs were activated with 10 μM norepinephrine at $t = 0$ s.

βγ interaction with lipid membranes is the rate-limiting step in translocation. We tested this hypothesis by mutating residues immediately upstream of the prenylated cysteine in the C-terminal domain of γ-subunits and found that hydrophobic and basic residues in this domain determined the translocation kinetics and free βγ-shuttling rates. These residues produced similar trends for peptide dissociation from lipid vesicles in vitro, suggesting that they interact directly with lipid membranes. Thus, G-protein signaling leverages subunit-dependent membrane affinities to differentially control βγ-translocation rates. Together with the highly conserved nature of these residues across species (39), this finding suggests that differential intermembrane movement may have been a key determinant in the evolution of γ-subunit C-terminal sequences. This raises the intriguing possibility that these sequences evolved on the basis of their interactions with membrane lipids rather than specific protein–protein interactions.

The basic lysine and hydrophobic phenylalanine residues in the C-terminal domain of slow-translocating γ-subunits are not essential for stable heterotrimer binding to the plasma membrane; rather, they influence membrane dissociation kinetics of free βγ-subunits. The role of the basic residues in the C-terminal domain of γ-subunits differs from that of polybasic regions commonly used to target prenylated proteins to the plasma membrane. For example, the C-terminal domain of KRas includes a region of six consecutive lysines. As a result, KRas associates strongly with negatively charged membranes and localizes preferentially to the plasma membrane, where the membrane potential is most negative (16). This strong membrane potential-sensing ability of polybasic domains requires more positively charged residues than are present in the γ–C-terminal domain (40). The two lysine residues in the γ-subunit KKFFC-GerGer motif, shown here to substantially enhance membrane binding, thus influence translocation kinetics but are unlikely to impart any strong preference for binding to the plasma membrane over other intracellular membranes.

Similar to G-protein heterotrimers, many small G proteins are both prenylated and palmitoylated (31). Heterotrimers are distinct, however, because the palmitoylated α-subunit and the prenylated βγ-complex can dissociate. For small G proteins such as HRas and NRas, both lipid modifications occur on a single protein (31). Analogous to how βγ redistributes over intracellular membranes on dissociation from the palmitoylated and/or myristoylated α-subunit, HRas and NRas redistribute from the plasma membrane to intracellular membranes following enzyme-catalyzed depalmitoylation (41). For both βγ and Ras, this movement is independent of active vesicular transport and likely proceeds by diffusion through the cytosol (6, 42). An important difference is that the βγ-complex can rapidly relocalize to the plasma membrane by binding α_{GDP} following receptor deactivation, whereas HRas and NRas cycle back to the plasma membrane along the secretory pathway following repalmitoylation at the Golgi (41). This difference illustrates how similar combinations of membrane-targeting motifs can be coupled in strikingly different ways to generate distinct patterns of protein movement.

Chaperone proteins assist membrane dissociation of many prenylated monomeric G proteins and play important roles in their signaling (22, 43). For example, guanine nucleotide dissociation inhibitors (GDIs) and GDI displacement factors (GDFs) work to control intermembrane movement of Rho and Rab GTPases in a manner that is regulated by the nucleotide-bound state of the G protein (20, 44). Interestingly, because βγ movement depends on its dissociation from activated α, it can be regulated by the GTP hydrolysis cycle of the α-subunit independent of the need for chaperones. The GDI-like solubilizing factor PDEδ acts independently of the nucleotide-bound state to facilitate intermembrane movement of Ras and serves a critical role in maintaining proper spatial organization and signaling of Ras (22, 43). Similar chaperones may also exist for βγ-subunits. Phosducin has been reported to facilitate βγ-translocation in photoreceptor cells (23), but more general roles and other specific βγ-chaperones have not been identified. In vitro membrane dissociation rates for peptides corresponding to the C-terminal domain of the γ-subunit are qualitatively consistent with the possibility that βγ movement between membranes in living cells occurs spontaneously via thermally stimulated detachment of free βγ from membranes. More specifically, our results suggest that γ-dependent differences in βγ-translocation rates can be explained by membrane affinities without an inherent need to invoke any γ-dependent interactions with chaperones.

Substantial evidence indicates that the differential translocation kinetics measured in our live cell assays reflect the native movement of endogenous βγ-subunits. Fast-, intermediate-, and slow-translocating γ-subunit types exhibit strikingly consistent translocation kinetics across a wide range of expression levels. This finding provides evidence that differential βγ-translocation rates are not a result of saturation of hypothetical binding sites at the plasma membrane due to overexpression of GFP-γ, but rather reflect the properties of endogenous γ-subunits. This conclusion is also supported by previous evidence that GFP-β1 translocation rates in different cell types depend on the native γ-subunit type that is predominantly expressed in a particular cell type (8).

The ability of βγ-dimers to translocate with differential kinetics suggests that the intracellular movement of G-protein subunits following heterotrimer activation can have important effects on downstream responses. G-protein α- and βγ-subunits were classically thought to act only at the plasma membrane, but recent findings suggest important new roles for G-protein subunits at intracellular locations (45–47). Whereas rapid diffusion of second messengers generated by G-protein effectors at the

plasma membrane enables fast signal communication to other regions of the cell, βγ translocation to intracellular regions could enable more specific communication between the plasma membrane and internal membranes. Differential translocation raises the possibility that temporal control over the activation of intracellular effectors can be governed by the βγ-subunit translocation kinetics. Unlike the α-subunit, the βγ-dimer has no intrinsic "off" switch other than reassociation with α_{GDP}. It is therefore possible that slow-translocating βγ-dimers remain active on intracellular membranes well after receptor deactivation, whereas signaling by fast-translocating βγ terminates more rapidly. The first-in, first-out reversible nature of βγ translocation could thus result in a first-on, first-off sequential activation of intracellular effectors preferentially activated by fast- vs. slow-translocating βγ-subunits. Hundreds of signaling pathways use heterotrimeric G proteins, and the differential kinetics of intracellular movement of G-protein subunits, mediated by differential membrane affinity, may play a critical role in determining signal-specific downstream responses.

Methods

Clones and Cell Lines. G-protein subunits were cloned into pcDNA 3.1 (Invitrogen), except for β1. which was cloned into pCMVBsd (Invitrogen). Untagged α- and β-subunits and FP-tagged wild-type γ-subunits have been described before (4, 6). GFP-tagged mutant γ-subunits were generated using a Quick Change II site-directed mutagenesis kit (Agilent). The $Venus_{1-155}$-γ subunits have been described previously (8). A PCR product of the C terminus of Venus (156–239) (KpnI on the 5′ end and BamHI on the 3′ end) and a full-length β2 (BamHI on the 5′ end and XhoI on the 3′ end) were ligated and inserted into the KpnI and XhoI sites of pcDNA3.1 to make the $Venus_{156-239}$-β2 construct. Venus and β2 were separated by a GGSGGG spacer. The human D1 dopamine receptor cDNA was from UMR cDNA Resource Center. The HeLa cell line was obtained from ATCC and cultured in MEM supplemented with 10% (vol/vol) dialyzed FBS (Atlanta Biologicals) and 1× antibiotic–antimycotic solution (CellGro) at 37 °C and 5% CO_2. Cells were cultured and transiently transfected in 29-mm glass-bottom culture dishes (In Vitro Scientific), using Lipofectamine 2000 (Invitrogen) and 1 μg of DNA corresponding to each transfected subunit. The studies of the effect of expression levels on translocation rates used dishes transfected with 1 μg, 0.3 μg, or 0.1 μg GFP-γ plasmid DNA. Before imaging, the cell medium was replaced with Hank's Buffered Salt Solution (CellGro) supplemented with 1 g/L glucose.

Live Cell Imaging. All imaging was performed using an Andor-Leica spinning disk confocal imaging system consisting of a Leica DMI 6000B microscope with adaptive focus control, a Yokogawa CSU ×1 spinning disk confocal unit, a FRAP-photoactivation unit, and an Andor iXon EMCCD camera. Solid-state lasers with wavelengths of 488 nm and 515 nm were used for excitation of GFP and YFP, respectively. Emission filters (Semrock) were GFP, 515/20; and YFP, 528/20. A single confocal plane was imaged at a rate of one frame every 3 s, and agonist/antagonist was added between frames at times specified in Figs. 1, 2, and 4. Endogenous α2AR activation was controlled with 10 μM (+)-norepinephrine (Sigma) and 60 μM yohimbine (Sigma). Endogenous CXCR4 activation was controlled with 100 ng/mL SDF-1α (CXCL 12) (Sigma) and 20 μM AMD3100 (Sigma). Transfected D1 receptors were activated with 10 μM A68930. The studies of the effect of expression levels on translocation rates used the following camera settings: (*i*) 336-ms exposure time, EM gain = 200 for low expression levels; (*ii*) 86-ms exposure time, EM gain = 200 for intermediate levels of expression; and (*iii*) 86-ms exposure time, EM gain = 0 for high expression levels. Intensities from images captured with conditions *ii* and *iii* were multiplied by correction factors to permit direct comparison with images captured under condition *i*. The correction factors were obtained by comparing images of the same cell under two different camera settings.

Image Analysis. Image collection and analysis were performed using Andor iQ software. Intracellular and plasma membrane regions were manually selected as shown in Fig. 2*A*. Previously we have shown that the brightest regions of intracellular βγ fluorescence, like those selected for analysis here, typically colocalize with fluorescent Golgi markers (4–6). The mean intensity in these regions was quantified for each image in a given sequence, with an appropriate region in the same image used for background subtraction. To facilitate direct comparison of translocation kinetics across different cells and experiments, we defined "translocation" quantitatively as the increase in fluorescence intensity in the intracellular membrane region upon receptor activation, normalized by the maximum intensity reached in that region.

Peptide Synthesis and in Vitro Assays. Prenylated and cysteine *O*-methylated peptides, labeled at their N terminus with a fluorescent *S*-bimanylthioacetyl residue, were synthesized using solution-phase methods as described previously (10, 11, 48, 49). Briefly, Fmoc-FFC(trityl)-OMe, Fmoc-GGC(trityl)-OMe, and Fmoc-AAC(trityl)-OMe were first synthesized (via the appropriate dipeptide derivatives) from the appropriate Fmoc amino acids and *S*-tritylcysteine *O*-methyl ester, using (1-cyano-2-ethoxy-2-oxoethylidenaminooxy)dimethylaminomorpholinocarbenium hexafluorophosphate (COMU) as coupling reagent (50), and then *S*-deprotected with trifluoroacetic acid/triethylsilane (96/4 vol/vol, 1 h, 25 °C) and *S*-prenylated using farnesyl or geranylgeranyl bromide (10). The resulting prenylated tripeptides were extended to pentapeptides by further cycles of Fmoc deprotection and COMU-mediated coupling, using γ-2-phenylisopropyl and 4-methyltrityl protection for the side chains of glutamic acid and lysine residues, and then Fmoc deprotected and labeled on their N termini with the succinimidyl ester of *S*-bimanylthioacetic acid (10). Peptides incorporating lysine or glutamic acid residues were then finally treated with 1% trifluoroacetic acid/2% triethylsilane to remove side-chain protecting groups without modifying the prenyl residues (51).

Rate constants for desorption of fluorescent prenylated peptides from lipid vesicles were determined as described previously (10) by monitoring the rates of spontaneous transfer of the peptides from "donor" lipid vesicles of the indicated compositions (also incorporating 1.5 mol% of the nonexchangeable fluorescence quencher DABS-PC) to "acceptor" lipid vesicles of the same composition but lacking the quencher. Transfer rate constants were verified to be independent of the total vesicle concentration, as expected for a transfer process rate limited by dissociation of the prenylated peptides from the donor vesicles. Fluorescent prenylated peptides were also prepared with sequences AAAAC(prenyl)-OMe and AAFFC(prenyl)-OMe, corresponding to some of the other γ-subunit mutants used in the live cell experiments, but these peptides were prone to aggregation and could not be homogeneously incorporated into lipid vesicles to measure their desorption rates accurately.

Mathematical Model. The mathematical model comprised a set of coupled ordinary differential equations, largely following a previous treatment of G-protein kinetics (15), but modified to consider the plasma membrane (PM) and intracellular membranes (IMs) as two distinct compartments, and allowing exchange of free βγ between them,

$$\frac{d[\alpha GDP\_\beta\gamma]}{dt} = \frac{dn_1}{dt} = V_1 - V_2 \quad [1]$$

$$\frac{d[\beta\gamma_{PM}]}{dt} = \frac{dn_2}{dt} = V_2 - V_1 - V_4 \quad [2]$$

$$\frac{d[\alpha GTP]}{dt} = \frac{dn_3}{dt} = V_2 - V_3 \quad [3]$$

$$\frac{d[\alpha GDP]}{dt} = \frac{dn_4}{dt} = V_3 - V_1 \quad [4]$$

$$\frac{d[\beta\gamma_{IM}]}{dt} = \frac{dn_5}{dt} = V_4, \quad [5]$$

where V_1 is the rate of heterotrimer reassociation, V_2 is the rate of heterotrimer activation/dissociation, V_3 is the rate of GAP-induced GTP hydrolysis, and V_4 is the rate of βγ exchange between the plasma membrane and intracellular membranes. These rates are given by the equations

$$V_1 = k_{ass}[\alpha GDP][\beta\gamma_{PM}] = k_{ass} n_4 n_2 \quad [6]$$

$$V_2 = \frac{k_{diss}[\alpha GDP\_\beta\gamma][R^*]}{K_2 + [\alpha GDP\_\beta\gamma]} = \frac{n_1 k_{diss}[R^*]}{K_2 + n_1} \quad [7]$$

$$V_3 = \frac{k_{hydr}[\alpha GTP][GAP]}{K_3 + \alpha GTP} = \frac{n_3 k_{hydr}[GAP]}{K_3 + n_3} \quad [8]$$

$$V_4 = k_{in}[\beta\gamma_{PM}] - k_{out}[\beta\gamma_{IM}] = k_{in} n_2 - k_{out} n_5, \quad [9]$$

where the enzymatic reactions corresponding to receptor-stimulated G-protein activation/dissociation and GAP accelerated GTP hydrolysis were

assumed to obey Michaelis–Menten kinetics with Michaelis–Menten constants K_2 and K_3, respectively. Other parameters in Eqs. **6**–**9** include rate constants for heterotrimer association (k_{ass}), heterotrimer dissociation (k_{diss}), and GTP hydrolysis (k_{hydr}). Conservation of the total number of G-protein subunits requires

$$[\beta\gamma_{TOTAL}] = [\alpha GDP\_\beta\gamma] + [\beta\gamma_{PM}] + [\beta\gamma_{ER}] = n_1 + n_2 + n_5 = constant = M \quad [10]$$

$$[\alpha_{TOTAL}] = [\alpha GDP\_\beta\gamma] + [\alpha GDP] + [\alpha GTP] = n_1 + n_3 + n_4 = constant = N. \quad [11]$$

Applying Eqs. **10** and **11**, we rewrite Eqs. **6**–**9** as

$$V_1 = k_{ass} n_2 (N + n_2 + n_5 - (M + n_3)) \quad [12]$$

$$V_2 = k_{diss}[R^*] \frac{M - (n_2 + n_5)}{K_2 + M - (n_2 + n_5)} \quad [13]$$

$$V_3 = k_{hydr}[GAP] \frac{n_3}{K_3 + n_3} \quad [14]$$

$$V_4 = k_{in} n_2 - k_{out} n_5. \quad [15]$$

The coupled Eqs. **1**–**5**, with values for V1–V4 substituted from Eqs. **12**–**15**, were solved using the "odeint" function in SciPy. Aside from k_{in} and k_{out}, all parameters were fixed at values previously used to simulate the "canonical mode" of G-protein signaling (15): $[\alpha_{TOTAL}] = [\beta\gamma_{TOTAL}] = 500$ nM with the initial condition that all subunits are in GDP heterotrimers; [R*] = 30 nM; [GAP] = 20 nM; $k_{ass} = 0.01$ nM^{-1}·s^{-1}, $k_{diss} = 20$ s^{-1}, $k_{hydr} = 5$ s^{-1}; and $K_2 = 500$ nM, $K_3 = 2$ nM.

ACKNOWLEDGMENTS. We thank L. Giri for discussions. This work was supported by National Institutes of Health Grants GM069027 and GM080558 (to N.G.) and National Research Service Award Postdoctoral Fellowship GM099351 (to P.R.O.).

1. Vartak N, Bastiaens P (2010) Spatial cycles in G-protein crowd control. *EMBO J* 29(16): 2689–2699.
2. Fivaz M, Meyer T (2005) Reversible intracellular translocation of KRas but not HRas in hippocampal neurons regulated by Ca2+/calmodulin. *J Cell Biol* 170(3):429–441.
3. Hamm HE (1998) The many faces of G protein signaling. *J Biol Chem* 273(2):669–672.
4. Akgoz M, Kalyanaraman V, Gautam N (2004) Receptor-mediated reversible translocation of the G protein betagamma complex from the plasma membrane to the Golgi complex. *J Biol Chem* 279(49):51541–51544.
5. Azpiazu I, Akgoz M, Kalyanaraman V, Gautam N (2006) G protein betagamma11 complex translocation is induced by Gi, Gq and Gs coupling receptors and is regulated by the alpha subunit type. *Cell Signal* 18(8):1190–1200.
6. Saini DK, Kalyanaraman V, Chisari M, Gautam N (2007) A family of G protein βγ subunits translocate reversibly from the plasma membrane to endomembranes on receptor activation. *J Biol Chem* 282(33):24099–24108.
7. Digby GJ, Sethi PR, Lambert NA (2008) Differential dissociation of G protein heterotrimers. *J Physiol* 586(14):3325–3335.
8. Karunarathne WKA, O'Neill PR, Martinez-Espinosa PL, Kalyanaraman V, Gautam N (2012) All G protein betagamma complexes are capable of translocation on receptor activation. *Biochem Biophys Res Commun* 421(3):605–611.
9. Wedegaertner PB, Wilson PT, Bourne HR (1995) Lipid modifications of trimeric G proteins. *J Biol Chem* 270(2):503–506.
10. Shahinian S, Silvius JR (1995) Doubly-lipid-modified protein sequence motifs exhibit long-lived anchorage to lipid bilayer membranes. *Biochemistry* 34(11):3813–3822.
11. Silvius JR, l'Heureux F (1994) Fluorimetric evaluation of the affinities of isoprenylated peptides for lipid bilayers. *Biochemistry* 33(10):3014–3022.
12. Silvius JR, Bhagatji P, Leventis R, Terrone D (2006) K-ras4B and prenylated proteins lacking "second signals" associate dynamically with cellular membranes. *Mol Biol Cell* 17(1):192–202.
13. Akgoz M, Kalyanaraman V, Gautam N (2006) G protein betagamma complex translocation from plasma membrane to Golgi complex is influenced by receptor gamma subunit interaction. *Cell Signal* 18(10):1758–1768.
14. Simonds WF, Butrynski JE, Gautam N, Unson CG, Spiegel AM (1991) G-protein beta gamma dimers. Membrane targeting requires subunit coexpression and intact gamma C-A-A-X domain. *J Biol Chem* 266(9):5363–5366.
15. Katanaev VL, Chornomorets M (2007) Kinetic diversity in G-protein-coupled receptor signalling. *Biochem J* 401(2):485–495.
16. Leventis R, Silvius JR (1998) Lipid-binding characteristics of the polybasic carboxy-terminal sequence of K-ras4B. *Biochemistry* 37(20):7640–7648.
17. Bhagatji P, Leventis R, Rich R, Lin CJ, Silvius JR (2010) Multiple cellular proteins modulate the dynamics of K-ras association with the plasma membrane. *Biophys J* 99(10):3327–3335.
18. Kosloff M, Alexov E, Arshavsky VY, Honig B (2008) Electrostatic and lipid anchor contributions to the interaction of transducin with membranes: Mechanistic implications for activation and translocation. *J Biol Chem* 283(45):31197–31207.
19. Nenninger A, Mastroianni G, Mullineaux CW (2010) Size dependence of protein diffusion in the cytoplasm of Escherichia coli. *J Bacteriol* 192(18):4535–4540.
20. Garcia-Mata R, Boulter E, Burridge K (2011) The 'invisible hand': Regulation of RHO GTPases by RHOGDIs. *Nat Rev Mol Cell Biol* 12(8):493–504.
21. Pfeffer S, Aivazian D (2004) Targeting Rab GTPases to distinct membrane compartments. *Nat Rev Mol Cell Biol* 5(11):886–896.
22. Ismail SA, et al. (2011) Arl2-GTP and Arl3-GTP regulate a GDI-like transport system for farnesylated cargo. *Nat Chem Biol* 7(12):942–949.
23. Sokolov M, et al. (2004) Phosducin facilitates light-driven transducin translocation in rod photoreceptors. Evidence from the phosducin knockout mouse. *J Biol Chem* 279 (18):19149–19156.
24. Murray D, McLaughlin S, Honig B (2001) The role of electrostatic interactions in the regulation of the membrane association of G protein beta gamma heterodimers. *J Biol Chem* 276(48):45153–45159.
25. Johnson JE, Cornell RB (1999) Amphitropic proteins: Regulation by reversible membrane interactions (review). *Mol Membr Biol* 16(3):217–235.
26. Escribá PV, et al. (2008) Membranes: A meeting point for lipids, proteins and therapies. *J Cell Mol Med* 12(3):829–875.
27. Casar B, et al. (2009) Ras subcellular localization defines extracellular signal-regulated kinase 1 and 2 substrate specificity through distinct utilization of scaffold proteins. *Mol Cell Biol* 29(5):1338–1353.
28. von Kriegsheim A, et al. (2009) Cell fate decisions are specified by the dynamic ERK interactome. *Nat Cell Biol* 11(12):1458–1464.
29. Kholodenko BN, Hancock JF, Kolch W (2010) Signalling ballet in space and time. *Nat Rev Mol Cell Biol* 11(6):414–426.
30. Cho WH, Stahelin RV (2005) Membrane-protein interactions in cell signaling and membrane trafficking. *Annu Rev Biophys Biomol Struct* 34:119–151.
31. Resh MD (2006) Trafficking and signaling by fatty-acylated and prenylated proteins. *Nat Chem Biol* 2(11):584–590.
32. Cadwallader KA, Paterson H, Macdonald SG, Hancock JF (1994) N-terminally myristoylated Ras proteins require palmitoylation or a polybasic domain for plasma membrane localization. *Mol Cell Biol* 14(7):4722–4730.
33. Hancock JF, Paterson H, Marshall CJ (1990) A polybasic domain or palmitoylation is required in addition to the CAAX motif to localize p21ras to the plasma membrane. *Cell* 63(1):133–139.
34. Resh MD (1996) Regulation of cellular signalling by fatty acid acylation and prenylation of signal transduction proteins. *Cell Signal* 8(6):403–412.
35. Schroeder H, et al. (1997) S-Acylation and plasma membrane targeting of the farnesylated carboxyl-terminal peptide of N-ras in mammalian fibroblasts. *Biochemistry* 36(42): 13102–13109.
36. Michaelson D, Ahearn I, Bergo M, Young S, Philips M (2002) Membrane trafficking of heterotrimeric G proteins via the endoplasmic reticulum and Golgi. *Mol Biol Cell* 13(9):3294–3302.
37. Takida S, Wedegaertner PB (2003) Heterotrimer formation, together with isoprenylation, is required for plasma membrane targeting of Gbetagamma. *J Biol Chem* 278(19): 17284–17290.
38. Marrari Y, Crouthamel M, Irannejad R, Wedegaertner PB (2007) Assembly and trafficking of heterotrimeric G proteins. *Biochemistry* 46(26):7665–7677.
39. Gautam N, Downes GB, Yan K, Kisselev O (1998) The G-protein betagamma complex. *Cell Signal* 10(7):447–455.
40. Yeung T, et al. (2006) Receptor activation alters inner surface potential during phagocytosis. *Science* 313(5785):347–351.
41. Rocks O, et al. (2005) An acylation cycle regulates localization and activity of palmitoylated Ras isoforms. *Science* 307(5716):1746–1752.
42. Goodwin JS, et al. (2005) Depalmitoylated Ras traffics to and from the Golgi complex via a nonvesicular pathway. *J Cell Biol* 170(2):261–272.
43. Chandra A, et al. (2012) The GDI-like solubilizing factor PDEδ sustains the spatial organization and signalling of Ras family proteins. *Nat Cell Biol* 14(2):148–158.
44. DerMardirossian C, Bokoch GM (2005) GDIs: Central regulatory molecules in Rho GTPase activation. *Trends Cell Biol* 15(7):356–363.
45. Saini DK, et al. (2010) Regulation of Golgi structure and secretion by receptor-induced G protein βγ complex translocation. *Proc Natl Acad Sci USA* 107(25):11417–11422.
46. Cho JH, Saini DK, Karunarathne WKA, Kalyanaraman V, Gautam N (2011) Alteration of Golgi structure in senescent cells and its regulation by a G protein γ subunit. *Cell Signal* 23(5):785–793.
47. Hewavitharana T, Wedegaertner PB (2012) Non-canonical signaling and localizations of heterotrimeric G proteins. *Cell Signal* 24(1):25–34.
48. Xue CB, Ewenson A, Becker JM, Naider F (1990) Solution phase synthesis of Saccharomyces cerevisiae a-mating factor and its analogs. *Int J Pept Protein Res* 36(4): 362–373.
49. Xue CB, Becker JM, Naider F (1991) Synthesis of S-alkyl and C-terminal analogs of the Saccharomyces cerevisiae a-factor. Influence of temperature on the stability of Fmoc and OFm groups toward HF. *Int J Pept Protein Res* 37(6):476–486.
50. El-Faham A, Subirós Funosas R, Prohens R, Albericio F (2009) COMU: A safer and more effective replacement for benzotriazole-based uronium coupling reagents. *Chemistry* 15(37):9404–9416.
51. Kadereit D, Deck P, Heinemann I, Waldmann H (2001) Acid-labile protecting groups for the synthesis of lipidated peptides. *Chemistry* 7(6):1184–1193.